Atmospheric Environment xxx (2014) 1–11

Contents lists available at ScienceDirect

Atmospheric Environment

journal homepage: www.elsevier.com/locate/atmosenv

Differences in satellite-derived NO_x emission factors between Eurasian and North American boreal forest fires

S.F. Schreier [a, b, *], A. Richter [a], D. Schepaschenko [b], A. Shvidenko [b], A. Hilboll [a], J.P. Burrows [a]

[a] Institute of Environmental Physics, University of Bremen, Germany
[b] International Institute for Applied Systems Analysis, Laxenburg, Austria

HIGHLIGHTS

- A satellite-based approach to estimate NO_x EFs for boreal forests is presented.
- The results indicate differences between Eurasian and North American boreal forests.
- Our EFs are in good agreement with recent reported values.
- However, EFs applied in frequently used emission inventories are 3–5 times larger.

ARTICLE INFO

Article history:
Received 1 April 2014
Received in revised form
26 August 2014
Accepted 27 August 2014
Available online xxx

Keywords:
Satellite measurements
Tropospheric NO_2
Fire radiative power
NO_x emission factor
Boreal forest

ABSTRACT

Current fire emission inventories apply universal emission factors (EFs) for the calculation of NO_x emissions over large biomes such as boreal forest. However, recent satellite-based studies over tropical and subtropical regions have indicated spatio-temporal variations in EFs within specific biomes. In this study, satellite measurements of tropospheric NO_2 vertical columns (TVC NO_2) from the GOME-2 instrument and fire radiative power (FRP) from MODIS are used for the estimation of fire emission rates (FERs) of NO_x over Eurasian and North American boreal forests. The retrieval of TVC NO_2 is based on a stratospheric correction using simulated stratospheric NO_2 instead of applying the reference sector method, which was used in a previous study. The model approach is more suitable for boreal latitudes. TVC NO_2 and FRP are spatially aggregated to a $1^\circ \times 1^\circ$ horizontal resolution and temporally averaged to monthly values. The conversion of the satellite-derived tropospheric NO_2 columns into production rates of NO_x from fire (P_f) is based on the NO_2/NO_x ratio as obtained from the MACC reanalysis data set and an assumed lifetime of NO_x. A global land cover map is used to define boreal forests across these two regions in order to evaluate the FERs of NO_x for this biome. The FERs of NO_x, which are derived from the gradients of the linear relationship between P_f and FRP, are more than 30% lower for North American than for Eurasian boreal forest fires. We speculate that these discrepancies are mainly related to the variable nitrogen content in plant tissues, which is higher in deciduous forests dominating large parts in Eurasia. In order to compare the obtained values with EFs found in the literature, the FERs are converted into EFs. The satellite-based EFs of NO_x are estimated at 0.83 and 0.61 g kg^{-1} for Eurasian and North American boreal forests, respectively, which is in good agreement with the value found in a recent emission factor compilation. However, recent fire emission inventories are based on EFs of NO_x that are 3–5 times larger, which indicates that there are still large uncertainties in estimates of NO_x from biomass burning, especially on the regional scale.

1. Introduction

Boreal forest, commonly referred to as taiga, is one of the largest terrestrial biomes and covers about 30% of the total global forest area (Pan et al., 2011). The taiga is dominated by evergreen (coniferous) and deciduous forests storing large amounts of

* Corresponding author. Institute of Environmental Physics, University of Bremen, Otto-Hahn-Allee 1, D-28359 Bremen, Germany.
E-mail address: schreier@iup.physik.uni-bremen.de (S.F. Schreier).

http://dx.doi.org/10.1016/j.atmosenv.2014.08.071
1352-2310/

nitrogen (N), which is an essential nutrient for all living organisms. However, wildfires across these ecosystems release large masses of N in form of nitrogen oxides ($NO_x = NO + NO_2$) and ammonia (NH_3) by flaming and smoldering fires, respectively, and affect the biosphere and atmosphere.

In general, the total amount of emissions released from boreal forest fires is relatively low compared to tropical and subtropical vegetation fires (Lobert et al., 1999). However, during exceptional climatic years such boreal forest fires can spread over large areas. Interestingly, Wooster and Zhang (2004) found that the intensity of fires is generally lower in Russian boreal forests than in North American boreal forests, and relate this difference to the respective dominance of surface fires in Russia and crown fires in North America.

Current model estimates of future fire regimes in the boreal zone predict a doubling of the number of wildfires by the end of the 21st century, an increase in the occurrence of catastrophic fires and fires that escape from control, a substantial increase of the burning severity, and changes in the intensity and gas composition of fire emissions caused by increased soil burning (Flannigan et al., 2009). Moreover, Shvidenko et al. (2011) suggested a linkage between catastrophic fires and large scale atmospheric anomalies for recent exceptionally large wildfires (e.g. fires in the Russian Far East vs. flooding in China in 2003; fires in European Russia vs. flooding in Pakistan and India in 2010). Thawing permafrost and the following drying up of typical landscapes in higher latitudes could lead to a dramatic loss of forested areas (Shvidenko and Schepaschenko, 2013). The increasing occurrence of catastrophic boreal wildfires in the future is likely to have an impact on air pollution and atmospheric chemistry. Therefore, accurate estimates of current fire emissions are needed to better understand the increasing future role of boreal forest fires. This can only be achieved by reducing uncertainties in fire emission estimates.

During the burning process, the nitrogen bound in the fuel is converted in part into oxides and N present in amino acids is converted to NO. However, NO_x may also result from the reaction of molecular nitrogen (N_2) with O_2 from the atmosphere at very high temperatures (Andreae and Merlet, 2001). While the higher thermal energy during the flaming stage leads to the break-up of plant materials into simpler N molecules enabling a full oxidation to NO_x, smoldering fires are rather incomplete. Chen et al. (2010) have examined the combustion efficiency by laboratory-controlled combustion experiments. Their results show that the fuel moisture content decreases the combustion efficiency and prolongs the smoldering phase before flames start. Emission factors (EFs) of NO_x, which are used in bottom-up emission inventories for the translation of biomass burned into trace gas emissions, can consequently change as a function of the fuel moisture content.

The amount of NO_x emissions being released from forest fires also depends on the N content in plant tissues. For boreal forest plants, this content varies substantially and depends on species, plant part burned, site productivity, geographical location, and other factors. For instance, in Siberian dark coniferous forests (dominated by *Pinus sibirica*, *Abies sibirica*, *Picea excelsa* and *Picea obovata*) of the southern taiga zone, the N content varies in the range of 0.1–0.45% (of dry matter mass) in stem wood, 0.5–1.0% in branches, 0.8–1.8% in needles, 0.3–0.9% in bark, and 0.4–1.2% in roots (Protopopov, 1975). Similar relative amounts are found for light coniferous forests (Rodin and Bazilevich, 1965; Bazilevich and Rodin, 1971). In the taiga of West Siberia, lichens contain 0.5%, mosses 0.9%, and grasses 1.1–2.0% of N (Bakhnov, 2001). The results of a study in northern Alberta suggest that deciduous forests (mainly trembling aspen) have a higher N content than coniferous (mainly white spruce) and mixed forests (Jerabkova et al., 2006). Although the differences in total litter mass and total N content in the canopy are negligible between the three forest types, the input of leaves and/or needles in terms of mass and N content is higher in deciduous stands. Moreover, it was shown that the nitrogen fraction in the observed smoke plume differs considerably among various fuel types burned in laboratory-controlled combustion experiments. While the concentration ratio of NO_x to grand total carbon (including C in CO_2, CO, and $PM_{2.5}$) is higher than 20% for litter, it is less than 10% for other fuel types such as leaves and stems (Chen et al., 2010). The results described above clearly indicate that the amounts of fuel nitrogen in the vegetation are rather heterogeneous throughout the taiga. Consequently, the EF of NO_x can vary within the boreal forest due to a changing N content in different tree species and fuel types that are burned.

There has been much discussion about the leading cause of NO_x emissions from wildfires. Andreae and Merlet (2001) suggest that temperatures in typical wildfires are not high enough to produce large amounts of NO_x via the oxidation of N_2. Nevertheless, the production of NO_x is more efficient during the flaming combustion. The fraction of reactive nitrogen in volatilized fuel nitrogen emitted accounts for 25–50%, with NO_x and NH_3 being the dominant reactive nitrogen species during flaming and smoldering combustion, respectively (Goode et al., 2000; Yokelson et al., 2008). In comparison, up to 50% of the fuel nitrogen might be converted into N_2 (Lobert et al., 1990). However, the exact mechanism of N_2 formation remains unclear as the detection of N_2 from open fires is influenced by the large N_2 fraction of the ambient air. For example, Mebust and Cohen (2013) found a seasonal cycle in NO_x emissions from African woody savanna fires, but could only speculate about the exact mechanisms.

The composition of total reactive nitrogen oxides (NO_y) in the continental troposphere mainly consists of nitric acid (HNO_3) and peroxyacyl nitrates (PANs), whereas NO_x constitutes only 15% (Singh et al., 2007). Smaller NO_x/NO_y fractions of 5% (spring) and 10% (summer) were derived from in-situ measurements taken during the ARCTAS (Arctic Research of the Composition of the Troposphere from Aircraft and Satellites) airborne campaigns in the high northern latitudes (Singh et al., 2010). Nevertheless, it was shown that the relatively small amount of NO_x can be transported into remote areas where it leads to a significant increase of O_3 (Singh et al., 2007). This can be explained by the efficient ozone production at low NO_x levels (Jacob, 1993). Val Martin et al. (2008) have shown that boreal wildfire emissions were responsible for higher levels of NO_x in remote areas downwind from the boreal region. They further concluded that the NO_x background levels during such fires were increased, and thus, the tropospheric O_3 budget was affected over large parts of the northern hemisphere.

Recent fire emission inventories are based on the translation of estimated biomass burned into trace gas emissions by applying uniform EFs for a relatively small number of biomes (e.g. Van Der Werf et al., 2010; Kaiser et al., 2012). However, more recent satellite-based studies have indicated substantial spatio-temporal variations of NO_x EFs within a specific biome and between different regions (Mebust and Cohen, 2013; Castellanos et al., 2014; Schreier et al., 2014). As the bulk of these results are confined to tropical and subtropical regions, we here expand this research to higher latitudes and estimate fire emission rates (FERs) and EFs of NO_x for boreal forests.

The following Sect. 2 gives a description of satellite measurements used in this study and outlines the approach to estimate FERs and EFs of NO_x from these measurements. The results are presented and discussed in Sect. 3. An overview on possible uncertainties in the approach is given in Sect. 4, followed by a summary and conclusions in Sect. 5.

Please cite this article in press as: Schreier, S.F., et al., Differences in satellite-derived NO_x emission factors between Eurasian and North American boreal forest fires, Atmospheric Environment (2014), http://dx.doi.org/10.1016/j.atmosenv.2014.08.071

2. Data retrieval and data analysis

2.1. Satellite measurements of NO_2

Measurements from the GOME-2 instrument on board the MetOp-A satellite (Callies et al., 2004) are used for the retrieval of tropospheric NO_2. The retrieval is based on the Differential Optical Absorption Spectroscopy (DOAS) method, which is described in detail elsewhere (Platt and Stutz, 2008). Here, we follow the retrieval approach as described in Richter et al. (2011) and Schreier et al. (2014). Briefly, the slant column densities (SCDs) are retrieved from the GOME-2 spectral measurements by fitting the absorption cross section of NO_2 and other trace gases in the spectral window between 425 and 497 nm. Instead of applying the reference sector method (Richter and Burrows, 2002), the stratospheric influence on the total column measurements has been estimated using stratospheric NO_2 fields simulated by the Bremen 3d CTM (B3dCTM) and scaled to observations over the Pacific.

The B3dCTM is a combined model approach based on the "Bremen transport model" (Sinnhuber et al., 2003a) and the chemistry code of the "Bremen two-dimensional model of the stratosphere and mesosphere" (Sinnhuber et al., 2003b; Winkler et al., 2008), which evolved from SLIMCAT (Chipperfield, 1999). B3dCTM is driven by ECMWF ERA Interim meteorological reanalysis fields (Dee et al., 2011). The detailed model setup is described in Hilboll et al. (2013b). The simulated stratospheric profiles are interpolated in space and time for each satellite measurement to yield stratospheric vertical columns and airmass factors (AMFs) (Hilboll et al., 2013a).

The impact of clouds on the retrieval of NO_2 is accounted for by removing measurements with a cloud fraction larger than 20%, based on the FRESCO+ retrieval (Wang et al., 2008). Finally, the SCDs are converted into vertical column densities (VCDs) by dividing through an AMF, which corrects for the different sensitivity of the measurements in different altitudes. A detailed description of the AMFs used in this study can be found in Nüß (2005) and Richter et al. (2005). The final retrieved tropospheric NO_2 vertical columns (TVC NO_2) are binned to a horizontal resolution of $1^\circ \times 1^\circ$ in order to reduce the effect of horizontal transport of NO_2.

Uncertainties in tropospheric NO_2 slant columns originating from the stratospheric correction are usually up to 5×10^{14} molec cm^{-2}, but can be as large as 2.5×10^{15} molec cm^{-2} at high latitudes in winter (Hilboll et al., 2013a). Due to the absence of fires in winter, however, these larger uncertainties are not of relevance for this study. The satellite-based retrieval of TVC NO_2 is affected by uncertainties, which are mainly caused by the conversion of SCDs into VCDs by applying AMFs (Boersma et al., 2004). A priori information used for the calculation of AMFs introduces the bulk of these uncertainties into the retrieval of TVC NO_2. For instance, inaccurate a priori information on aerosols can have a substantial influence on the accuracy of the AMFs, and thus, on the precision of TVC NO_2. The vertical position of the aerosol layer relative to the NO_2 layer is of particular interest. While the measurement sensitivity of the instrument is reduced when the aerosol layer is located above the NO_2 plume, it is increased when aerosols are located within or below the NO_2 plume (Leitão et al., 2010). A decrease (increase) in the measurement sensitivity by not correctly accounting for the aerosol information would lead to an overestimation (underestimation) of the AMFs, and thus, to an underestimation (overestimation) of TVC NO_2. Besides the location of the aerosol layer, uncertainties in aerosol amounts and optical properties can also deteriorate the accuracy of TVC NO_2. Leitão et al. (2010) have shown that the effect of a varying single scattering albedo (SSA) on the AMF can be larger than 70% for polluted atmospheres.

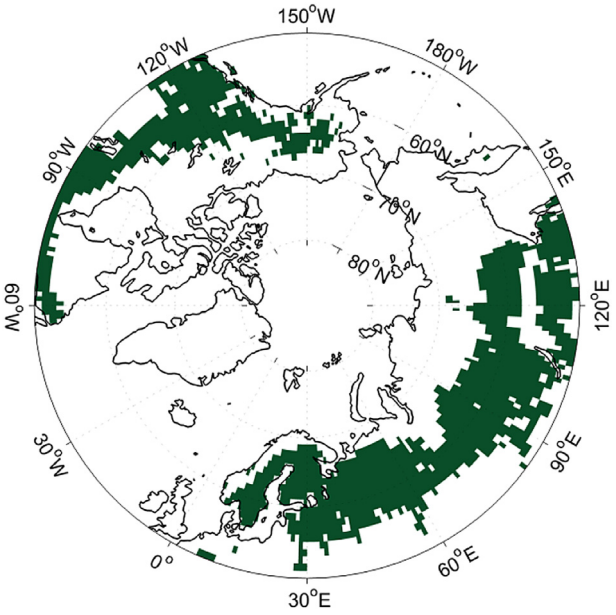

Fig. 1. Boreal forests in Eurasia and North America as defined by the aggregation of evergreen needleleaf forest, deciduous needleleaf forest, mixed forest, and woody savannas on a grid of $1^\circ \times 1^\circ$ horizontal resolution (see Table 1) using the UMD classification scheme (Hansen et al., 2000; Friedl et al., 2010).

2.2. Satellite measurements of fire radiative power

Fire radiative power (FRP) is a measure for the power radiated from a fire in terms of its temperature, based on the black body concept described by the Stefan–Boltzmann law (Kaufman et al., 1998). MODIS observations on board the near-polar orbiting satellites Terra (10:30 LT) and Aqua (13:30 LT) are available since 1999 and 2002, respectively. Amongst other parameters, FRP is retrieved from these measurements at a 1 km^2 horizontal resolution. According to the equatorial overpass time of the GOME-2 instrument (9:30 LT), we make use of the MOD14CM FRP product from the Terra satellite (10:30 LT), provided at a $1^\circ \times 1^\circ$ horizontal resolution (ftp://neespi.gsfc.nasa.gov/data/s4pa/Fire/MOD14CM1.005/).

2.3. Global land cover map

The Collection 5 MODIS Global Land Cover Type product (Friedl et al., 2010), which is available at https://lpdaac.usgs.gov/products/modis_products_table/mcd12q1, is used for the definition of boreal forests. According to the horizontal resolution selected for TVC NO_2 and FRP, the land cover product is spatially aggregated to $1^\circ \times 1^\circ$ by applying a majority filter. The 14-class University of Maryland classification (UMD) is used to define boreal forest pixels (Hansen et al., 2000). The aggregation of $1^\circ \times 1^\circ$ pixels covered by coniferous forests, deciduous forests, or a mixture of both form the basis of the estimation of FERs and EFs of NO_x for boreal forests in Eurasia and North America. In the UMD classification, woody savanna is defined as a mixture of trees (40–60%) and grassland. As woody savannas cover considerable areas in Alaska, Russia, and Scandinavia, and in order to increase the data points used for the estimation of FERs of NO_x, we included woody savannas in the definition of boreal forest pixels. The aggregation of the four land cover types (evergreen needleleaf forest, deciduous needleleaf forest, mixed forest, and woody savannas) between 50°N and 80°N is shown in Fig. 1 and the definition of the regions Eurasia and North America is highlighted in Table 1.

Please cite this article in press as: Schreier, S.F., et al., Differences in satellite-derived NO_x emission factors between Eurasian and North American boreal forest fires, Atmospheric Environment (2014), http://dx.doi.org/10.1016/j.atmosenv.2014.08.071

2.4. Satellite measurements of aerosol optical depth

In order to assess the possible influence of aerosols on the retrieval of TVC NO_2, and thus, on the magnitude of the estimated FERs and EFs of NO_x for boreal forests in Eurasia and North America, we have analyzed the aerosol optical depth (AOD) and vertical profiles of wildfire emissions for these regions. The AOD is a parameter describing the column integrated extinction over the entire atmosphere and is derived from MODIS spectral measurements between 470 and 2130 nm (Remer et al., 2008). The aerosol product from MODIS on board Terra at 550 nm is used to evaluate the possible relative influence of the AOD on the retrieval of TVC NO_2 between the Eurasian and North American boreal forest pixels. The AOD product has been downloaded from ftp://ladsweb.nascom.nasa.gov/allData/51/MOD08_M3/2005/.

2.5. Vertical profiles of wildfire emissions

A 4-dimensional data set of fire smoke with a resolution of $1^\circ \times 1^\circ \times 500$ m has been recently calculated by Sofiev et al. (2013). The estimated vertical profiles are based on a semi-empirical formula for the plume-top height, satellite observations of active fires, and meteorological conditions derived from a numerical weather prediction model. The vertical profiles are available for the entire globe and cover the whole time period analyzed in this study (2007–2012). These data are used to deduce the possible role of a variable mean injection height on the retrieval of TVC NO_2 between the two regions.

2.6. An adapted approach for the boreal region

In general, fire emission inventories (e.g. GFEDv3.1 and GFASv1.0) estimate the total amount of NO_x (usually reported as NO) released by fires. As satellite instruments, such as GOME-2, measure NO_2, the conversion of TVC NO_2 into production rates of NO_x from fire (P_f) is a further step to prepare the data for the analysis.

The aim of this study is the satellite-based estimation of FERs and EFs of NO_x for the Eurasian and North American boreal forests. As recent satellite-based studies have indicated substantial spatio-temporal variations in EFs for African (Mebust and Cohen, 2013) and South American (Castellanos et al., 2014) biomes, we hypothesize that EFs could also fluctuate among the large taiga forests.

We build on the approach described in Schreier et al. (2014) to estimate linear gradients between P_f and FRP, here referred to as FERs of NO_x. The assumption made for the following approach is that the fire radiative power is mainly related to the amount of fuel burned and not to the temperature of the individual fire. The amount of NO_x emitted in turn is assumed to be linearly related to the amount of fuel burned.

We start the analysis with evaluating the temporal correlation between the gridded monthly mean TVC NO_2 and FRP for the boreal forest pixels. Schreier et al. (2014) have indicated strong correlation for larger regions located in the tropics and subtropics. However, they also pointed out the comparatively weak correlation between the two parameters for higher latitudes. One possible reason for the weaker correlation is related to the fact that the bulk of boreal forest fires are generally smaller in size (e.g. Stocks et al., 2003) when compared to the rather extensive slash and burn activities in Africa and South America. As a result, the measurement sensitivity of the satellite instrument might be too low for the detection of NO_2 produced from such smaller fires. Another possible explanation for the weak correlations found by Schreier et al. (2014) could be the larger uncertainty in tropospheric NO_2 vertical columns in higher latitudes, which are introduced by the stratospheric correction method used in their study. Basically, the applied reference sector method assumes that there are no tropospheric sources of NO_x over a specific and rather remote region over the Pacific and that the stratospheric NO_2 column varies only with latitude, but not with longitude. However, these assumptions can introduce negative NO_2 columns by overestimating the stratospheric NO_2, especially in higher latitudes mainly during winter and spring. Hilboll et al. (2013a) suggest that these negative NO_2 columns could be related to the polar vortex and the resulting zonal inhomogeneity. In order to improve the quality of TVC NO_2 over the boreal regions, we use stratospheric NO_2 columns as calculated by the B3dCTM simulations in this study (see Sect. 2.1).

Using the linear relationship between TVC NO_2 and FRP (see Eq. (1)), the y-intercepts are subtracted from the TVC NO_2 (see Eq. (2)). This step is performed to isolate the tropospheric NO_2 column contribution produced by fire (TVC$_f$ NO_2), assuming that y-intercepts represent the NO_2 background (TVC$_b$ NO_2) and that there is no or a negligible small seasonal cycle in NO_2 background.

$$\mathrm{TVC}[\mathrm{NO_2}] = \mathrm{slope}*\mathrm{FRP} + \mathrm{TVC_b}[\mathrm{NO_2}] \quad (1)$$

$$\mathrm{TVC_f}[\mathrm{NO_2}] = \mathrm{TVC}[\mathrm{NO_2}] - \mathrm{TVC_b}[\mathrm{NO_2}] \quad (2)$$

In a second step, the obtained monthly gridded values of TVC$_f$ NO_2 (in units of 10^{15} molec cm^{-2}) are then converted into monthly gridded values of NO_x production rates P_f (in units of g NO_x s^{-1}) (see Eq. (3)).

$$P_f = \frac{\mathrm{TVC_f}[\mathrm{NO_2}]*M\left(1+\frac{\mathrm{NO}}{\mathrm{NO_2}}\right)A_p}{N_A*\tau}, \quad (3)$$

where TVC$_f$ NO_2 is the number density of NO_2 molecules produced by fires integrated over the tropospheric vertical column (in

Table 1
Selected regions and land cover types with their respective share of the total boreal forest area. The land cover types are used to define boreal forests in Eurasia and North America (see Sect. 2.3).

Region	Latitudes	Longitudes	Land cover types[a]	Share of total area[b]	Share of total area[c]
Eurasia	50°–80°N	0°–180°E	Evergreen needleleaf forest	7.1%	0.5%
			Deciduous needleleaf forest	17.6%	31.2%
			Mixed forest	53.7%	39.8%
			Woody savannas	21.6%	28.5%
North America	50°–80°N	170°–35°W	Evergreen needleleaf forest	57.6%	59.3%
			Mixed forest	12.2%	9.3%
			Woody savannas	30.2%	31.4%

[a] Based on the Collection 5 MODIS Global Land Cover Type product (UMD classification).
[b] Percentages represent share of total boreal forest area as defined in this study and shown in Fig. 1.
[c] Percentages represent share of total boreal forest area remaining after data filtering (see Fig. 3).

Please cite this article in press as: Schreier, S.F., et al., Differences in satellite-derived NO_x emission factors between Eurasian and North American boreal forest fires, Atmospheric Environment (2014), http://dx.doi.org/10.1016/j.atmosenv.2014.08.071

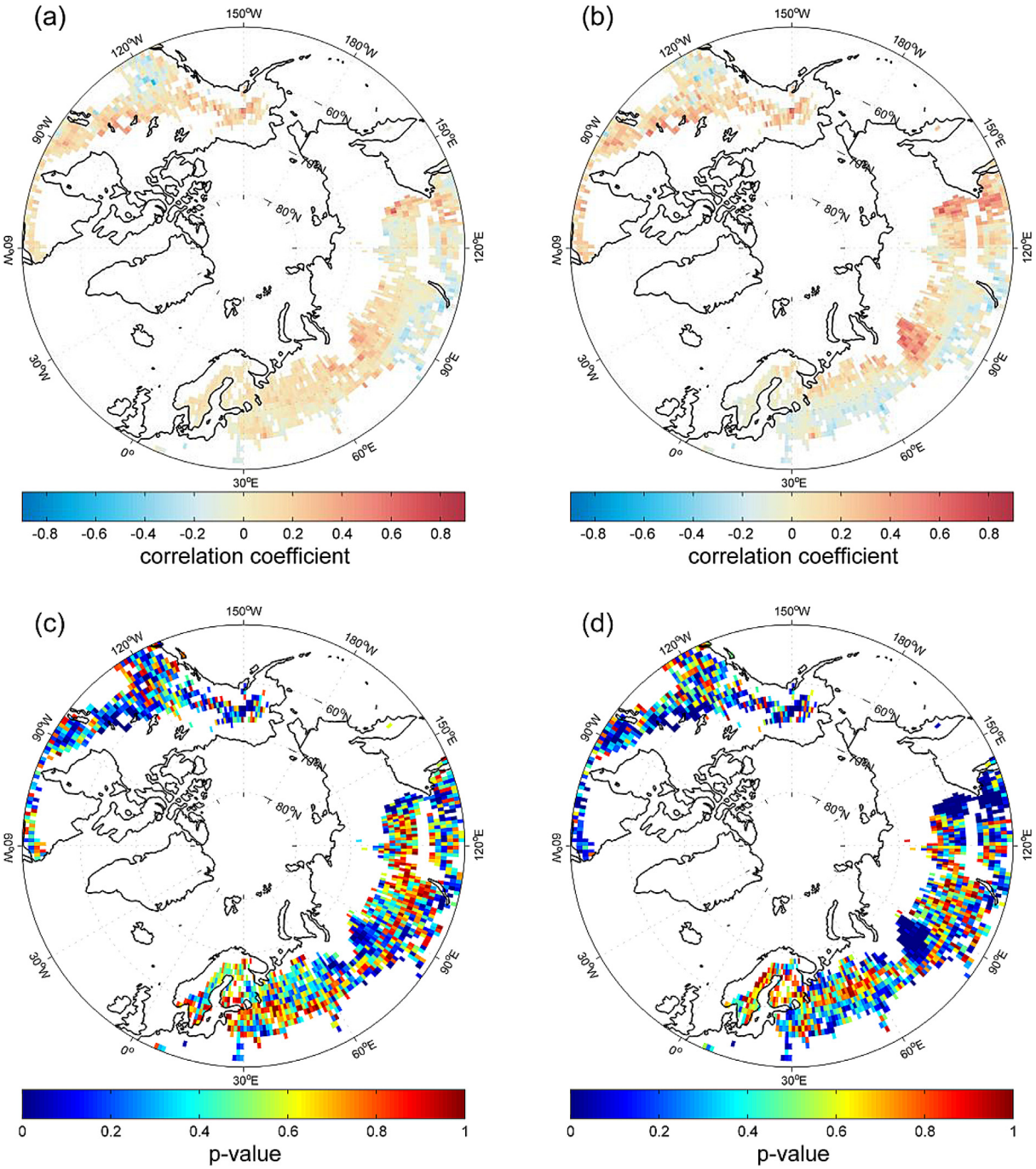

Fig. 2. Correlation coefficients (r) of the linear regression (see Eq. (1)) of TVC NO_2 against FRP (upper) and statistical significance (lower) for the period 2007–2012. A p-value smaller than 0.05 means that the correlation is statistically significant within a 95% confidence level. The retrieval of TVC NO_2 is based on the removal of stratospheric NO_2 applying the reference sector (a) and (c) as well as using B3dCTM simulations (b) and (d). All colored $1^\circ \times 1^\circ$ pixels are defined as boreal forest (see Fig. 1 and Table 1).

molecules cm^{-2}) and M is the molar mass of NO (in g mol^{-1}). The term $1 + NO/NO_2$ accounts for the NO_2/NO_x ratio (without units) as derived from the MACC reanalysis data set (see below) and A_p is the respective pixel area (in cm^2). N_A denotes Avogadro's number (in molecules mol^{-1}) and τ is the assumed lifetime of NO_x (in seconds). We use a constant value of 6 h for τ, which is based on the findings of Beirle et al. (2011) for the megacity Moscow and Takegawa et al. (2003) for biomass burning plumes over northern Australia. According to the described conversion of TVC NO_2, the FRP values have also been multiplied by A_p. Further details about the conversion are given in Schreier et al. (2014).

A detailed description of the MACC data assimilation system for chemically reactive gases, which is based on ECMWF IFS and MOZART-3 CTM simulations, can be found in Inness et al. (2013). We have calculated daily weighted averages of the NO_2/NO_x ratio for the 8 given UT hours (3, 6, 9, 12, 15, 18, 21, and 0 UT) by including 29 hybrid sigma-pressure levels between the surface and ~10 km altitude to reflect tropospheric values. We have then interpolated between these UT hours by including daily gridded maps of the geographical location of the GOME-2 overpass time (UT) to construct daily values of the NO_2/NO_x ratio. Finally, we have computed monthly means of the NO_2/NO_x ratio with a horizontal

Please cite this article in press as: Schreier, S.F., et al., Differences in satellite-derived NO_x emission factors between Eurasian and North American boreal forest fires, Atmospheric Environment (2014), http://dx.doi.org/10.1016/j.atmosenv.2014.08.071

resolution of 1° × 1° for the entire period (2007–2012). These values are included in the formula (Eq. (3)) for the conversion of TVC NO_2 into P_f, instead of assuming a constant value for the NO_2/NO_x ratio as done in Schreier et al. (2014). Although there is no systematic difference in the results when using the gridded values of NO_2/NO_x ratio obtained from the MACC reanalysis data instead of a constant value of 0.75 (not shown), we use these values as they account for the seasonal variability.

A linear regression model is used for the calculation of gradients between P_f and FRP for all boreal forest pixels with a correlation coefficient (r) between TVC NO_2 and FRP higher than 0.3. As the major parts of boreal forests examined in this study are located in rather remote areas, we have tested whether the population density filter as applied in Schreier et al. (2014) is crucial for this study. We found that this filter has no significant effect on the obtained results (not shown) and have therefore not applied such filtering.

In short, the approach to estimate FERs of NO_x is similar to the approach used by Schreier et al. (2014), but three parameters have been modified for this study. Firstly, TVC NO_2 is based on a stratospheric correction using model simulations to reduce the uncertainty from stratospheric NO_2. Secondly, monthly gridded maps of the NO_2/NO_x ratio derived from the MACC reanalysis data are used to account for seasonality and spatial variation of this ratio. Thirdly, filtering by population density data has been omitted as it proved to be not necessary.

3. Results and discussion

3.1. Statistical evaluation of regression coefficients

The correlation coefficients as calculated from the pixel-wise linear relationship between monthly means of TVC NO_2 and FRP are shown in Fig. 2 for the entire boreal forest (as defined in Fig. 1). The correlation coefficients as computed in Schreier et al. (2014) by applying the reference sector method for the retrieval of TVC NO_2 (a) are compared with the correlation coefficients based on the new TVC NO_2 as computed by subtracting the B3dCTM simulated stratospheric NO_2 (b). There is some degree of improvement, especially in the Far East Russia and parts of Siberia, due to the improved stratospheric correction of the NO_2 satellite measurements. Negative correlation coefficients indicate the influence of anthropogenic emissions, which are higher during winter months despite the absence of fires. As already stated in Schreier et al. (2014), negative values are not included in the approach to derive FERs of NO_x. In order to give evidence about the statistical significance, p-values have been computed for the linear relationship between TVC NO_2 (based on the reference sector method (c) and simulated stratospheric NO_2 (d)) and FRP (see Eq. (1)). The adapted approach used in this study for the evaluation of FERs and EFs of NO_x in the boreal region clearly increases the number of pixels with p-values <0.05 (statistical significance within a 95% confidence level). There are fewer pixels having correlation coefficients >0.3 in the boreal region when compared to tropical and subtropical regions (Schreier et al., 2014). This might be related to the fact that there are many smaller fires with NO_2 signals falling below the detection limit of GOME-2. Although large fires account for over 85% of the total area burned in the Canadian boreal forest, they account for less than 5% of the fires (Stocks et al., 2003). Therefore, we anticipate that the estimation of FERs and EFs of NO_x is based on rather larger forest fires in this study. The gradients of the linear regression model used for estimating fire emission rates are calculated for those 1° × 1° pixels having p-values <0.05 and correlation coefficients $r > 0.3$. By this data selection, we focus on areas where there is a clear link between satellite observed fires and satellite retrieved NO_2 columns. As shown in Fig. 3, the number of boreal forest pixels used for the estimation of FERs of NO_x is reduced by these thresholds to 141 and 63 for Eurasia and North America, respectively. Although a correlation coefficient of 0.3 is not high, it is statistically significant in our study, even for the relatively low amount of data points available in the selected time series. The use of a higher threshold value (e.g. $r > 0.4$) would lead to an even smaller data set, which would not be beneficial for the analysis. Therefore, we feel confident to use the above mentioned threshold values ($r > 0.3$ and p-values < 0.05) for this study.

In Fig. 3, the y-intercepts of the linear regressions (see Eq. (1)) are shown for the selected boreal forest pixels, based on the filter criteria (p-value < 0.05 and $r > 0.3$). These values reveal useful information about the background level of tropospheric NO_2 in the selected areas as they reflect levels of tropospheric NO_2 produced from other NO_x sources than fire. The y-intercept values are subtracted from the TVC NO_2 grid cells to obtain the tropospheric NO_2 produced from fire (TVC_f NO_2), which is used for the conversion of TVC NO_2 into P_f (see Eq. (2) and Sect. 2.6). The subtraction of these values is performed under the assumption that there is no seasonal cycle in background tropospheric NO_2.

3.2. Determination of fire emission rates of NO_x

Scatter plots for the relationship between P_f and FRP are shown in Fig. 4 for Eurasia (red) and North America (blue). All boreal forest pixels with a p-value <0.05 and $r > 0.3$ are plotted in the graph. The total number of data points, i.e., TVC NO_2 averaged over one grid cell and one month, included in this plot is 6791 and 3298 for Eurasia and North America, respectively (see Table 2). A maximum

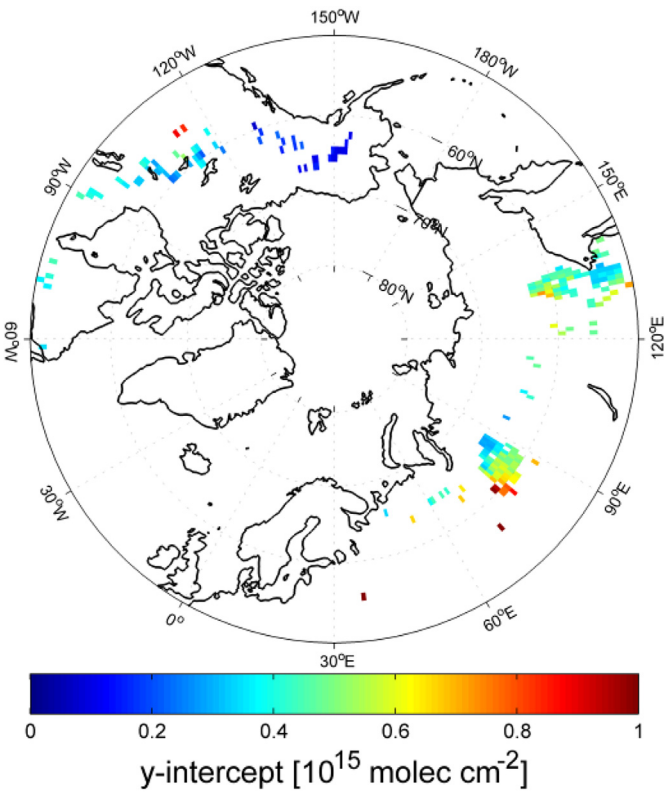

Fig. 3. Y-intercepts of the linear regression of TVC NO_2 against FRP for the six-year period (2007–2012). The y-intercepts representing the background levels in NO_2 columns are subtracted from the total tropospheric NO_2 columns (see Sect. 2.6). All pixels with a p-value <0.05 and $r > 0.3$ are shown in the Figure and used as a selection criterion for the estimation of FERs and EFs of NO_x.

Please cite this article in press as: Schreier, S.F., et al., Differences in satellite-derived NO_x emission factors between Eurasian and North American boreal forest fires, Atmospheric Environment (2014), http://dx.doi.org/10.1016/j.atmosenv.2014.08.071

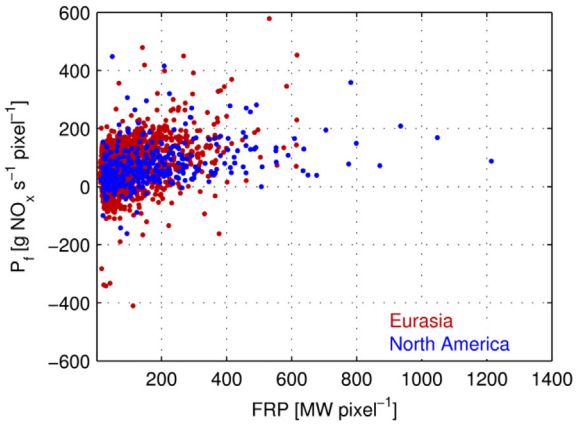

Fig. 4. Estimated productions rates of NO_x from fire (P_f) plotted against associated FRP values over boreal forests Eurasia (red) and North America (blue). All $1° \times 1°$ pixels with a p-value <0.05 and $r > 0.3$ are included in the plot (see Sect. 2.6). (For interpretation of the references to color in this figure legend, the reader is referred to the web version of this article.)

number of 72 data points would result for a single boreal forest pixel if the satellite instruments would have detected a signal for each month of the selected time period (2007–2012) for both TVC NO_2 and FRP. As boreal wildfires mainly occur in summer and to a lesser extent in spring and fall, the maximum number of data points for the individual pixels is reduced due to the absence of fires in winter. A division of the total number of data points (6791 and 3298) by the number of boreal forest pixels remaining after data filtering (141 and 63) results in average numbers (or months containing signals of both TVC NO_2 and FRP) of 48 and 52 for an individual pixel located in Eurasia and North America, respectively.

In general, a large spread of data is expected because of measurement uncertainties, the simplifications made in the conversion of NO_2 columns to NO_x production rates and from the horizontal and vertical changes of N and moisture contents in the vegetation (Fig. 4). For instance, a dry deciduous forest with increased N content will release more NO_x per unit FRP than a rather humid coniferous forest. There is a clear indication that single fire events can be more intensive in North America than in Russia. Wooster and Zhang (2004) suggest that the higher fire intensity in North American boreal forests is linked to more intensive crown fires.

In order to reduce the spread of data and exclude outliers, data points are averaged within consecutive FRP-intervals of 15 MW $pixel^{-1}$. The application of the binning method moreover leads to a result that represents spatio-temporally averaged FERs of NO_x for the respective region. Due to the larger amount of data available for Eurasia, the threshold criterion for the binning could be set to $\geq$10 data points available within the interval, whereas for North America it is set to $\geq$5.

Table 2
Spatio-temporally averaged fire emission rates (FERs) of NO_x in [g s^{-1} MW^{-1}] and emission factors (EFs) of NO_x in [g kg^{-1}] for the Eurasian and North American boreal forest fires analyzed in this study. FERs and EFs of NO_x are reported as NO. The approach to derive the FERs and EFs of NO_x is described in Sect. 2.6.

Region	N	FER[a]	r^2	EF[b]
Eurasia	6791	0.34 ± 0.03	0.87	0.83 ± 0.07
North America	3298	0.25 ± 0.03	0.79	0.61 ± 0.07

Uncertainty of FERs and EFs is given as the standard error of the slope as shown in Fig. 5.
[a] Derived by applying a binning procedure as described in the text.
[b] Based on the conversion factor of 0.41 kg MJ^{-1} as suggested by Vermote et al. (2009).

After binning, clear linear relationships are visible for both regions, albeit with different slopes. This result shows that there are differences in FERs of NO_x between the two selected regions with higher values observed for the Eurasian boreal forest fires (Fig. 5). In other words, the emissions of NO_x per unit of FRP are lower on average for forest fires in North America. One possible explanation could be the lower N content in evergreen (coniferous) species dominating large parts of the North American region (see Table 1 and Jerabkova et al., 2006). Moreover, Chen et al. (2010) have reported that the concentration ratio of NO_x over the grand total carbon is highest for litter combustion, which is more likely in deciduous forests dominating the Eurasian region analyzed in our study. Wooster and Zhang (2004) found an overall higher-temperature flaming combustion in North American boreal forests. Assuming that the production of NO_x via the oxidation of N_2 would be the dominant source of NO_x from boreal wildfires, higher FERs of NO_x would be expected for boreal forest fires in North America. As this is not the case in our study, we can only speculate that the observed differences in FERs of NO_x between Eurasian and North American boreal forests are rather related to the variable N content in plant tissues. We argue that the higher FERs of NO_x derived for the Eurasian boreal forests are likely attributed to the larger proportion of deciduous stands such as larch forests (Schepaschenko et al., 2011) and/or to the non-existence of such forests in North America. Large differences in the N content are especially found in the canopy litter, with ~30% larger amounts reported for deciduous forests (Jerabkova et al., 2006). In addition, the N content in grasses is higher than in other plant tissues (Bakhnov, 2001). Consequently, the dominance of surface fires in deciduous forests in Eurasia (see Wooster and Zhang, 2004) could explain the larger emissions of NO_x per unit of FRP.

3.3. Conversion into emission factors of NO_x

In order to compare our values with the values found in literature, the FERs are translated into EFs of NO_x by applying a

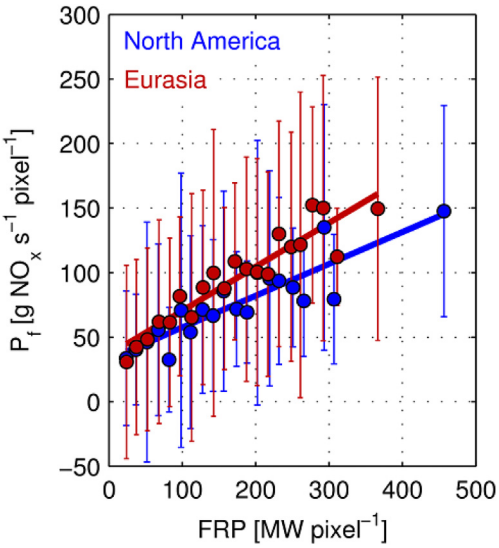

Fig. 5. Spatio-temporally averaged fire emission rates (FERs) of NO_x for boreal forest in Eurasia (red) and North America (blue) derived by applying a binning procedure as explained in Sect. 3.2. The gradients, here referred to as FERs, are calculated by applying a linear regression of monthly means of P_f against monthly means of FRP by including all pixels with a p-value <0.05 and $r > 0.3$. The error bars show one standard deviation of P_f values within the consecutive FRP-intervals. A summary of the statistics is given in Table 2. (For interpretation of the references to color in this figure legend, the reader is referred to the web version of this article.)

Please cite this article in press as: Schreier, S.F., et al., Differences in satellite-derived NO_x emission factors between Eurasian and North American boreal forest fires, Atmospheric Environment (2014), http://dx.doi.org/10.1016/j.atmosenv.2014.08.071

conversion factor of 0.41 kg MJ^{-1} as suggested by Vermote et al. (2009). The values for the spatio-temporally averaged FERs and EFs of NO_x, the total number of data points included in the analysis (N), and the coefficient of determination (r^2) are summarized in Table 2.

A comparison of the obtained EFs with the EF provided by Akagi et al. (2011) indicates very good agreement, as their reported value of 0.9 g kg^{-1} for the whole boreal forest biome is in good agreement with the value derived for the Eurasian boreal forest (0.83 g kg^{-1}) in our study. However, the EF estimated for the North American boreal forest (0.61 g kg^{-1}) is about 30% lower than the average value reported by Akagi et al. (2011). Wiedinmyer et al. (2006) have estimated fire emissions for North America by assigning EFs for each land cover type in the Global Land Cover (GLC2000) classification. The EFs of NO_x used in that study are in the range of 2.1–2.7 g kg^{-1} for sub-polar needleleaved and broadleaved forests and thus, around three times larger than the EFs obtained in our study. Van Der Werf et al. (2010) and Kaiser et al. (2012) applied constant values of 3.41 and 3.4 g NO_x kg^{-1}, respectively, for the entire extratropical forest biome. When compared to our values, their values are five times larger. As about 80% of global burned area is found in the tropics and subtropics (e.g. Van Der Werf et al., 2010), the given difference in EFs of NO_x for the boreal forest is less important for fire emission inventories on a global scale. However, this difference would affect the magnitude of fire emissions considerably on the regional level.

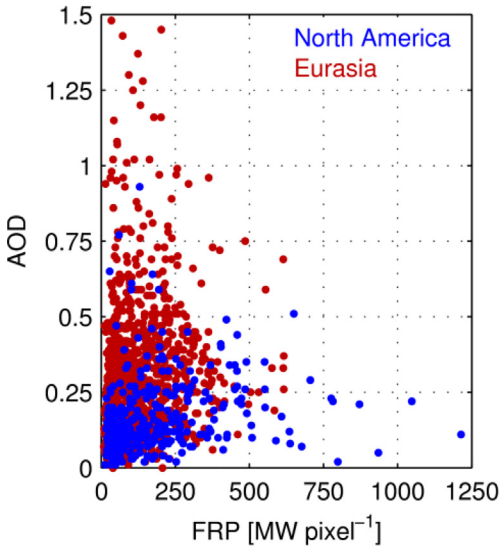

Fig. 6. Scatterplot between AOD and FRP for Eurasia (red) and North America (blue). The data points represent all boreal forest pixels (2007–2012) with a p-value < 0.05 and r > 0.3. (For interpretation of the references to color in this figure legend, the reader is referred to the web version of this article.)

4. Possible uncertainties in the approach

In order to make sure that the observed differences in FERs and EFs of NO_x between the two regions are related to characteristics of the vegetation and fire type, we analyze and discuss possible factors that could affect the retrieval of TVC NO_2 and the conversion into P_f. The bulk of uncertainties in the retrieval of TVC NO_2 results from the conversion of SCDs into VCDs by the use of AMFs (see Sect. 2.2). Here, we focus on the impact of aerosol amounts and properties as well as on injection profiles of fire smoke that could affect the magnitude of FERs of NO_x between Eurasia and North America differently. Additionally, the lifetime of NO_x and the NO_2/NO_x ratio are discussed in terms of possible relative influences on the conversion of TVC NO_2 into P_f between the two selected regions.

4.1. Impact of aerosol amounts and properties

First, the AOD retrieved from MODIS on board Terra (in accordance to the overpass time of GOME-2 on board MetOp-A) is analyzed over the Eurasian and North American boreal forests. In Fig. 6, the AOD is plotted against FRP for boreal forest pixels with a p-value <0.05 and r > 0.3 in Eurasia (red) and North America (blue). Clearly, the AOD is lower over North American forests when the FRP value of the respective pixel is lower than 500 MW. This might be an indication that aerosol amounts are largely dominated by fires in this region. In comparison, aerosols could be transported from anthropogenic emission sources (from coal, gas, and oil burning) into the Eurasian boreal forest pixels, as a certain proportion of data points indicate higher AOD values in Eurasia. In terms of AMF calculations, an increase in AOD generally results in higher measurement sensitivity when the aerosols are below or mixed with the NO_2 molecules, and thus, increase the AMF. A decreased AMF comes along with a reduced sensitivity due to the location of aerosols above the NO_2 plume (shielding effect). Stohl et al. (2013) highlighted the important role of black carbon emissions from gas flaring in the Arctic. According to their findings, black carbon emissions from gas flaring, especially in Russia, are transported into boreal forest pixels analyzed in our study. Black carbon is considered as a fine black fluffy particle with highly absorbing properties. Highly absorbing aerosols, either located above or mixed with the NO_2 molecules, can only reduce the measurement sensitivity, and thus, decrease the AMF. In order to assess the influence of the increased AOD over the Eurasian boreal forest pixels on the magnitude of TVC NO_2, it is important to know the relative location and the properties of the additional aerosol load in the troposphere. However, this information is still highly unknown as no accurate data sets for the selected regions are currently available. Thus, we can only speculate that the effect of an increased AOD could lead to an underestimation of the FERs and EFs of NO_x over Eurasia due to an overestimation of the AMF.

Secondly, the single scattering albedo (SSA) of aerosols and its possible impact on the retrieval of TVC NO_2 shall be discussed. The SSA describes the scattering and absorbing properties of aerosols and is simply defined as the ratio between scattering and extinction (scattering + absorption). While highly absorbing aerosols are characterized by a lower SSA, the SSA of highly scattering aerosols tends towards one. In general, a less complete combustion (smoldering fire) leads to a larger fine mode fraction of aerosols, which increases scattering, and thus, the SSA (Eck et al., 2009). Giles et al. (2012) have reported an average SSA of 0.95 at 440 nm for Bonanza Creek in Alaska. In contrast, the SSA in Western Siberia is estimated at 0.92–0.93 at 440 nm in an altitude between 500 and 2000 m, which is in good agreement with a measurement site at Tomsk (Panchenko et al., 2012). Both locations match with parts of the boreal forest pixels that are analyzed in this study. The lower SSA in Russia could be related to the influence of anthropogenic emissions sources in the vicinity of boreal forest pixels included in the analysis. However, a larger fraction of grasses burned could also contribute to the lower value. By assuming that the two reported SSA values are representative for the two selected regions, we conclude that the FERs of NO_x in Eurasia are rather underestimated than overestimated.

4.2. Impact of injection heights

The mean seasonal daytime injection profiles of the plumes from fires are shown in Fig. 7 over boreal forest fires in Eurasia (left)

Please cite this article in press as: Schreier, S.F., et al., Differences in satellite-derived NO_x emission factors between Eurasian and North American boreal forest fires, Atmospheric Environment (2014), http://dx.doi.org/10.1016/j.atmosenv.2014.08.071

and North America (right). As for the analysis of AOD, all boreal forest pixels with a p-value <0.05 and $r > 0.3$ are included in the computation of injection profiles as presented in Fig. 7. In general, the seasonal distribution of the injection profiles is similar in both regions with the highest injection heights observed in April, May, June, July, and August (see Sofiev et al., 2013), which is the main forest fire season. As the differences are very small, the relative effects on the retrieval of TVC NO_2 between the two regions are assumed to be negligibly small. Val Martin et al. (2010) found a quantitative link between median injection heights and FRP in North America. The slightly higher injection heights in North America could thus be related to the increased FRP values observed in this region when compared with maximum FRP values in Eurasia (see Fig. 4). Nevertheless, the higher injection heights observed over North American boreal forest fires could potentially result in an overestimation of the AMF. This can be explained by the fact that the measurement sensitivity, which is smallest close to the Earth's surface, is overestimated if the NO_2 plume is higher in the atmosphere than assumed (see Leitão et al., 2010). Therefore, FERs and EFs of NO_x in North America could potentially be overestimated relative to those in Eurasia.

4.3. Impact of NO_x lifetime and NO_2/NO_x ratio

With respect to the lifetime of NO_x and the NO_2/NO_x ratio, the influence of an increased NO_2 layer is twofold. While the lifetime of NO_x is slightly increased towards higher altitudes, the NO_2/NO_x ratio is decreased as the relative proportion of NO_2 decreases with increasing altitude. However, the changes are too small to expect a significant relative influence on the magnitude of FERs of NO_x between the two regions.

5. Summary and conclusion

In this study, the fire emission rates (FERs) and emission factors (EFs) of NO_x are estimated for boreal forest fires in Eurasia and North America, based on the empirical relationship between satellite-derived tropospheric NO_2 vertical columns (TVC NO_2) and fire radiative power (FRP). The retrieval of TVC NO_2 is based on a model-based correction of the stratosphere instead of the previously used reference sector method, which clearly improves the empirical relationship between TVC NO_2 and FRP at mid and high latitudes. As the GOME-2 retrievals provide NO_2 columns, a simplified formula including the lifetime of NO_x and the NO_2/NO_x ratio is used to convert tropospheric NO_2 column densities into production rates of NO_x from fire (P_f) in terms of mass concentrations. Instead of assuming a constant value of 0.75 for the NO_2/NO_x ratio (see Schreier et al., 2014), gridded values obtained from the MACC reanalysis data set are applied in this study. Although these monthly means account for the seasonal variability, no improvement was found for the empirical relationship.

The boreal forest pixels are defined according to the collection 5 MODIS global land cover product and confined between 50° and 80°N. The approach used to estimate FERs of NO_x only includes boreal forest pixels that exceed a value of 0.3 for the temporal correlation coefficient between TVC NO_2 and FRP and are statistically significant within a 95% confidence. This criterion has been chosen to exclude regions with an even weaker link between observed NO_2 columns and FRP, which are not beneficial for the analysis. On the other hand, a higher threshold value applied for the correlation coefficient (e.g. $r > 0.4$) decreases the available data points.

The spatio-temporally averaged FERs of NO_x are estimated at 0.34 and 0.25 g s^{-1} MW^{-1} for Eurasian and North American boreal forest fires, respectively. We speculate that the observed difference is related to changes in the N content and moisture conditions of the fuel types burned. Moreover, the type of fire (surface fires vs. crown fires) and the linked combustion of dead material on the ground and tops of trees could affect the magnitude of FERs.

For a better comparison with values found in the literature, the FERs are translated into EFs of NO_x by simply applying a conversion factor of 0.41 kg MJ^{-1}, assuming the findings by Vermote et al. (2009). The satellite-based values are estimated at 0.83 and 0.61 g kg^{-1} for Eurasian and North American boreal forests, respectively. A comparison with the emission factor reported by Akagi et al. (2011) for the entire boreal forest (0.9 g kg^{-1}) indicates good agreement. However, recent fire emission inventories have used EFs of NO_x that are 3–5 times larger. Our findings have possible implications for future estimates of fire emissions, especially on the regional scale where our results indicate less fire related NO_x emissions.

We discussed possible factors that could affect the observed differences in FERs and EFs of NO_x between North America and Eurasia and suggest that considering possible systematic biases in the NO_2 retrievals, the real differences of NO_x EFs between the two regions could even be larger. Therefore, we conclude that the observed differences of FERs and EFs of NO_x between Eurasia and North America are real and should be investigated by other, more direct methods in the future.

Acknowledgements

Parts of this study were performed while Stefan F. Schreier was participating in the Young Scientists Summer Program (YSSP) and working in collaboration with the Ecosystems Services and Management (ESM) Program at the International Institute for Applied

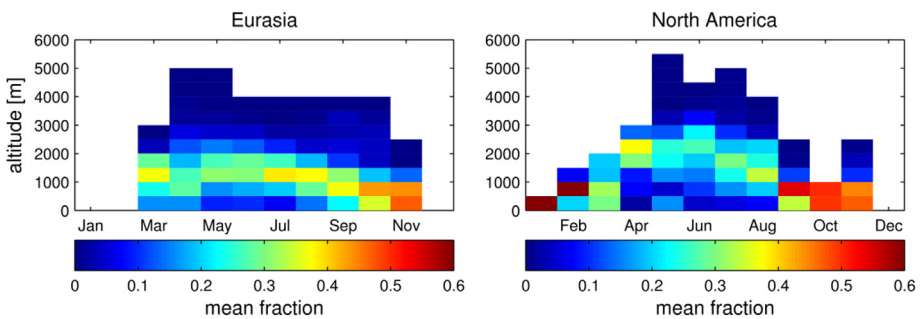

Fig. 7. Mean seasonal daytime injection profiles (Sofiev et al., 2013) over boreal forest fires in Eurasia (left) and North America (right). All boreal forest pixels (2007–2012) with a p-value < 0.05 and $r > 0.3$ are included in the averaging of injection profiles.

Please cite this article in press as: Schreier, S.F., et al., Differences in satellite-derived NO_x emission factors between Eurasian and North American boreal forest fires, Atmospheric Environment (2014), http://dx.doi.org/10.1016/j.atmosenv.2014.08.071

Systems Analysis (IIASA). Stefan F. Schreier wishes to acknowledge financial support provided by IIASA and the Earth System Science Research School (ESSReS), an initiative of the Helmholtz Association of German Research Centres (HGF) at the Alfred Wegener Institute for Polar and Marine Research (AWI). GOME-2 lv1 data have been provided by EUMETSAT. We thank NASA for the free use of the MODIS data and wish to thank M. Sofiev for providing the injection profiles. We gratefully acknowledge the MACC team and Anne Blechschmidt for providing the reanalysis data. Finally, we wish to thank two anonymous reviewers for their useful comments.

References

Akagi, S.K., Yokelson, R.J., Wiedinmyer, C., Alvarado, M.J., Reid, J.S., Karl, T., Crounse, J.D., Wennberg, P.O., 2011. Emission factors for open and domestic biomass burning for use in atmospheric models. Atmos. Chem. Phys. 11, 4039–4072. http://dx.doi.org/10.5194/acp-11-4039-2011.

Andreae, M.O., Merlet, P., 2001. Emission of trace gases and aerosols from biomass burning. Glob. Biogeochem. Cycles 15, 955–966.

Bakhnov, V.R., 2001. General scheme of evolution of swampy soils and swamps of taiga belt. In: Vasiliev, S.V., Titlyanova, A.A., Velichko, A.A. (Eds.), Weat Siberian Peatlands and Carbon Cycle: Past and Present. Institute of Soil Science and Agrochemistry, Siberian Branch of RAS, Novosibirsk, pp. 10–11.

Bazilevich, N.I., Rodin, L.E. (Eds.), 1971. Biological Productivity and Mineral Cycling in the Terrestrial Plant Communities. Nuka Publ., Leningrad, p. 313 (in Russian).

Beirle, S., Boersma, K.F., Platt, U., Lawrence, M.G., Wagner, T., 2011. Megacity emissions and lifetimes of nitrogen oxides probed from space. Science 333, 1737–1739.

Boersma, K.F., Eskes, H.J., Brinksma, E.J., 2004. Error analysis for tropospheric NO_2 retrieval from space. J. Geophys. Res. D Atmos. 109, D04311–04320.

Callies, J., Corpaccioli, E., Eisinger, M., Lefebvre, A., Munro, R., Perez-Albinana, A., Ricciarelli, B., Calamai, L., Gironi, G., Veratti, R., Otter, G., Eschen, M., Van Riel, L., 2004. GOME-2 ozone instrument on-board the European METOP satellites. In: Weather and Environmental Satellites, Proceedings of SPIE. The International Society for Optical Engineering, Denver, CO, pp. 60–70.

Castellanos, P., Boersma, K.F., Van Der Werf, G.R., 2014. Satellite observations indicate substantial spatiotemporal variability in biomass burning NO_x emission factors for South America. Atmos. Chem. Phys. 14, 3929–3943. http://dx.doi.org/10.5194/acp-14-3929-2014.

Chen, L.-W.A., Verburg, P., Shackelford, A., Zhu, D., Susfalk, R., Chow, J.C., Watson, J.G., 2010. Moisture effects on carbon and nitrogen emission from burning of wildland biomass. Atmos. Chem. Phys. 10, 6617–6625. http://dx.doi.org/10.5194/acp-10-6617-2010.

Chipperfield, M.P., 1999. Multiannual simulations with a three-dimensional chemical transport model. J. Geophys. Res. 104, 1781–1805.

Dee, D.P., Uppala, S.M., Simmons, A.J., Berrisford, P., Poli, P., Kobayashi, S., Andrae, U., Balmaseda, M.A., Balsamo, G., Bauer, P., Bechtold, P., Beljaars, A.C.M., van de Berg, L., Bidlot, J., Bormann, N., Delsol, C., Dragani, R., Fuentes, M., Geer, A.J., Haimberger, L., Healy, S.B., Hersbach, H., Hólm, E.V., Isaksen, L., Kållberg, P., Köhler, M., Matricardi, M., McNally, A.P., Monge-Sanz, B.M., Morcrette, J.-J., Park, B.-K., Peubey, C., de Rosnay, P., Tavolato, C., Thépaut, J.-N., Vitart, F., 2011. The ERA-Interim reanalysis: configuration and performance of the data assimilation system. Q. J. Roy. Meteorol. Soc. 137, 553–597. http://dx.doi.org/10.1002/qj.828.

Eck, T.F., Holben, B.N., Reid, J.S., Sinyuk, A., Hyer, E.J., O'Neill, N.T., Shaw, G.E., Vande Castle, J.R., Chapin, F.S., Dubovik, O., Smirnov, A., Vermote, E., Schafer, J.S., Giles, D., Slutsker, I., Sorokine, M., Newcomb, W.W., 2009. Optical properties of boreal region biomass burning aerosols in central Alaska and seasonal variation of aerosol optical depth at an Arctic coastal site. J. Geophys. Res. D Atmos. 114 http://dx.doi.org/10.1029/2008JD010870.

Flannigan, M.D., Krawchuk, M.A., De Groot, W.J., Wotton, B.M., Gowman, L.M., 2009. Implications of changing climate for global wildland fire. Int. J. Wildland Fire 18, 483–507. http://dx.doi.org/10.1071/WF08187.

Friedl, M.A., Sulla-Menashe, D., Tan, B., Schneider, A., Ramankutty, N., Sibley, A., Huang, X., 2010. MODIS collection 5 global land cover: algorithm refinements and characterization of new datasets. Remote Sens. Environ. 114, 168–182. http://dx.doi.org/10.1016/j.rse.2009.08.016.

Giles, D.M., Holben, B.N., Eck, T.F., Sinyuk, A., Smirnov, A., Slutsker, I., Dickerson, R.R., Thompson, A.M., Schafer, J.S., 2012. An analysis of AERONET aerosol absorption properties and classifications representative of aerosol source regions. J. Geophys. Res. D Atmos. 117 http://dx.doi.org/10.1029/2012JD018127.

Goode, J.G., Yokelson, R.J., Ward, D.E., Susott, R.A., Babbitt, R.E., Davies, M.A., Hao, W.M., 2000. Measurements of excess O_3, CO_2, CO, CH_4, C_2H_4, C_2H_2, HCN, NO, NH_3, HCOOH, CH_3COOH, HCHO, and CH_3OH in 1997 Alaskan biomass burning plumes by airborne Fourier transform infrared spectroscopy (AFTIR). J. Geophys. Res. 105, 22147–22166. http://dx.doi.org/10.1029/2000JD900287.

Hansen, M.C., Defries, R.S., Townshend, J.R.G., Sohlberg, R., 2000. Global land cover classification at 1 km spatial resolution using a classification tree approach. Int. J. Remote Sens. 21, 1331–1364.

Hilboll, A., Richter, A., Rozanov, A., Hodnebrog, Ø., Heckel, A., Solberg, S., Stordal, F., Burrows, J.P., 2013a. Improvements to the retrieval of tropospheric NO_2 from satellite – stratospheric correction using SCIAMACHY limb/nadir matching and comparison to Oslo CTM2 simulations. Atmos. Meas. Tech. 6, 565–584. http://dx.doi.org/10.5194/amt-6-565-2013.

Hilboll, A., Richter, A., Burrows, J.P., 2013b. Long-term changes of tropospheric NO_2 over megacities derived from multiple satellite instruments. Atmos. Chem. Phys. 13, 4145–4169. http://dx.doi.org/10.5194/acp-13-4145-2013.

Inness, A., Baier, F., Benedetti, A., Bouarar, I., Chabrillat, S., Clark, H., Clerbaux, C., Coheur, P., Engelen, R.J., Errera, Q., Flemming, J., George, M., Granier, C., Hadji-Lazaro, J., Huijnen, V., Hurtmans, D., Jones, L., Kaiser, J.W., Kapsomenakis, J., Lefever, K., Leitão, J., Razinger, M., Richter, A., Schultz, M.G., Simmons, A.J., Suttie, M., Stein, O., Thépaut, J.-N., Thouret, V., Vrekoussis, M., Zerefos, C., The MACC team, 2013. The MACC reanalysis: an 8 yr data set of atmospheric composition. Atmos. Chem. Phys. 13, 4073–4109. http://dx.doi.org/10.5194/acp-13-4073-2013.

Jacob, D.J., 1993. Factors regulating ozone over the United States and its export to the global atmosphere. J. Geophys. Res. 98, 14817–814826.

Jerabkova, L., Prescott, C.E., Kishchuk, B.E., 2006. Nitrogen availability in soil and forest floor of contrasting types of boreal mixedwood forests. Can. J. For. Res. 36, 112–122. http://dx.doi.org/10.1139/x05-220.

Kaiser, J.W., Heil, A., Andreae, M.O., Benedetti, A., Chubarova, N., Jones, L., Morcrette, J.J., Razinger, M., Schultz, M.G., Suttie, M., Van Der Werf, G.R., 2012. Biomass burning emissions estimated with a global fire assimilation system based on observed fire radiative power. Biogeosciences 9, 527–554. http://dx.doi.org/10.5194/bg-9-527-2012.

Kaufman, Y.J., Justice, C.O., Flynn, L.P., Kendall, J.D., Prins, E.M., Giglio, L., Ward, D.E., Menzel, W.P., Setzer, A.W., 1998. Potential global fire monitoring from EOS-MODIS. J. Geophys. Res. D Atmos. 103, 32215–32238.

Leitão, J., Richter, A., Vrekoussis, M., Kokhanovsky, A., Zhang, Q.J., Beekmann, M., Burrows, J.P., 2010. On the improvement of NO_2 satellite retrievals – aerosol impact on the airmass factors. Atmos. Meas. Tech. 3, 475–493. http://dx.doi.org/10.5194/amt-3-475-2010.

Lobert, J.M., Scharffe, D.H., Hao, W.M., Crutzen, P.J., 1990. Importance of biomass burning in the atmospheric budgets of nitrogen-containing gases. Nature 346, 552–554.

Lobert, J.M., Keene, W.C., Logan, J.A., Yevich, R., 1999. Global chlorine emissions from biomass burning: reactive Chlorine Emissions Inventory. J. Geophys. Res. D Atmos. 104, 8373–8389.

Mebust, A.K., Cohen, R.C., 2013. Observations of a seasonal cycle in NO_x emissions from fires in African woody savannas. Geophys. Res. Lett. 40, 1451–1455. http://dx.doi.org/10.1002/grl.50343.

Nüß, J.H., 2005. Improvements of the Retrieval of Tropospheric NO_2 from GOME and SCIAMACHY Data (Ph.D. thesis). University of Bremen.

Pan, Y., Birdsey, R.A., Fang, J., Houghton, R., Kauppi, P.E., Kurz, W.A., Phillips, O.L., Shvidenko, A., Lewis, S.L., Canadell, J.G., Ciais, P., Jackson, R.B., Pacala, S.W., McGuire, A.D., Piao, S., Rautiainen, A., Sitch, S., Hayes, D., 2011. A large and persistent carbon sink in the world's forests. Science 333, 988–993.

Panchenko, M.V., Zhuravleva, T.B., Terpugova, S.A., Polkin, V.V., Kozlov, V.S., 2012. An empirical model of optical and radiative characteristics of the tropospheric aerosol over West Siberia in summer. Atmos. Meas. Tech. 5, 1513–1527. http://dx.doi.org/10.5194/amt-5-1513-2012.

Platt, U., Stutz, J., 2008. Differential Optical Absorption Spectroscopy. Physics of Earth and Space Environments. Springer, Berlin.

Protopopov, V.V., 1975. Sredoobrazuiushchaia Rol' Temnokhvoinogo Lesa. Novosibirsk.

Remer, L.A., Kleidman, R.G., Levy, R.C., Kaufman, Y.J., Tanré, D., Mattoo, S., Martins, J.V., Ichoku, C., Koren, I., Yu, H., Holben, B.N., 2008. Global aerosol climatology from the MODIS satellite sensors. J. Geophys. Res. D Atmos. 113 http://dx.doi.org/10.1029/2007JD009661.

Richter, A., Burrows, J.P., 2002. Tropospheric NO_2 from GOME measurements. Adv. Space Res. 29, 1673–1683.

Richter, A., Burrows, J.P., Nüß, H., Granier, C., Niemeier, U., 2005. Increase in tropospheric nitrogen dioxide over China observed from space. Nature 437, 129–132. http://dx.doi.org/10.1038/nature04092.

Richter, A., Begoin, M., Hilboll, A., Burrows, J.P., 2011. An improved NO_2 retrieval for the GOME-2 satellite instrument. Atmos. Meas. Tech. 4, 1147–1159. http://dx.doi.org/10.5194/amt-4-1147-2011.

Rodin, L.E., Bazilevich, N.I., 1965. Dynamics of Organic Matter and Biological Turnover of Ash Constituents and Nitrogen in Major Types of Vegetation of the Globe. Academy of Sciences of the USSR, Moscow-Leningrad, p. 253 (in Russian).

Schepaschenko, D., McCallum, I., Shvidenko, A., Fritz, S., Kraxner, F., Obersteiner, M., 2011. A new hybrid land cover dataset for Russia: a methodology for integrating statistics, remote sensing and in situ information. J. Land Use Sci. 6, 245–259. http://dx.doi.org/10.1080/1747423X.2010.511681.

Schreier, S.F., Richter, A., Kaiser, J.W., Burrows, J.P., 2014. The empirical relationship between satellite-derived tropospheric NO_2 and fire radiative power and possible implications for fire emission rates of NO_x. Atmos. Chem. Phys. 14, 2447–2466. http://dx.doi.org/10.5194/acp-14-2447-2014.

Shvidenko, A.Z., Shchepashchenko, D.G., Vaganov, E.A., Sukhinin, A.I., Maksyutov, S.S., McCallum, I., Lakyda, I.P., 2011. Impact of wildfire in Russia between 1998–2010 on ecosystems and the global carbon budget. Dokl. Earth Sci. 441, 1678–1682. http://dx.doi.org/10.1134/S1028334X11120075.

Please cite this article in press as: Schreier, S.F., et al., Differences in satellite-derived NO_x emission factors between Eurasian and North American boreal forest fires, Atmospheric Environment (2014), http://dx.doi.org/10.1016/j.atmosenv.2014.08.071

Shvidenko, A.Z., Schepaschenko, D.G., 2013. Climate change and wildfires in Russia. Lesovedenie 5, 50–61. http://dx.doi.org/10.1134/S199542551307010X.

Singh, H.B., Salas, L., Herlth, D., Kolyer, R., Czech, E., Avery, M., Crawford, J.H., Pierce, R.B., Sachse, G.W., Blake, D.R., Cohen, R.C., Bertram, T.H., Perring, A., Wooldridge, P.J., Dibb, J., Huey, G., Hudman, R.C., Turquety, S., Emmons, L.K., Flocke, F., Tang, Y., Carmichael, G.R., Horowitz, L.W., 2007. Reactive nitrogen distribution and partitioning in the North American troposphere and lowermost stratosphere. J. Geophys. Res. D Atmos. 112 http://dx.doi.org/10.1029/2006JD007664.

Singh, H.B., Anderson, B.E., Brune, W.H., Cai, C., Cohen, R.C., Crawford, J.H., Cubison, M.J., Czech, E.P., Emmons, L., Fuelberg, H.E., Huey, G., Jacob, D.J., Jimenez, J.L., Kaduwela, A., Kondo, Y., Mao, J., Olson, J.R., Sachse, G.W., Vay, S.A., Weinheimer, A., Wennberg, P.O., Wisthaler, A., The ARCTAS Science Team, 2010. Pollution influences on atmospheric composition and chemistry at high northern latitudes: boreal and California forest fire emissions. Atmos. Environ. 44, 4553–4564. http://dx.doi.org/10.1016/j.atmosenv.2010.08.026.

Sinnhuber, B.-M., Weber, M., Amankwah, A., Burrows, J.P., 2003a. Total ozone during the unusual Antarctic winter of 2002. Geophys. Res. Lett. 30, 1580–1584. http://dx.doi.org/10.1029/2002GL016798.

Sinnhuber, M., Burrows, J.P., Chipperfield, M.P., Jackman, C.H., Kallenrode, M.-B., Künzi, K.F., Quack, M., 2003b. A model study of the impact of magnetic field structure on atmospheric composition during solar proton events. Geophys. Res. Lett. 30, 1818–1821. http://dx.doi.org/10.1029/2003GL017265.

Sofiev, M., Vankevich, R., Ermakova, T., Hakkarainen, J., 2013. Global mapping of maximum emission heights and resulting vertical profiles of wildfire emissions. Atmos. Chem. Phys. 13, 7039–7052. http://dx.doi.org/10.5194/acp-13-7039-2013.

Stocks, B.J., Mason, J.A., Todd, J.B., Bosch, E.M., Wotton, B.M., Amiro, B.D., Flannigan, M.D., Hirsch, K.G., Logan, K.A., Martell, D.L., Skinner, W.R., 2003. Large forest fires in Canada, 1959–1997. J. Geophys. Res. 108, 8149. http://dx.doi.org/10.1029/2001JD000484.

Stohl, A., Klimont, Z., Eckhardt, S., Kupiainen, K., Shevchenko, V.P., Kopeikin, V.M., Novigatsky, A.N., 2013. Black carbon in the Arctic: the underestimated role of gas flaring and residential combustion emissions. Atmos. Chem. Phys. 13, 8833–8855. http://dx.doi.org/10.5194/acp-13-8833-2013.

Takegawa, N., Kondo, Y., Koike, M., Ko, M., Kita, K., Blake, D.R., Nishi, N., Hu, W., Liley, J.B., Kawakami, S., Shirai, T., Miyazaki, Y., Ikeda, H., Russel-Smith, J., Ogawa, T., 2003. Removal of NOx and NOy in biomass burning plumes in the boundary layer over northern Australia. J. Geophys. Res. Atmos. 108, 4308. http://dx.doi.org/10.1029/2002jd002505.

Val Martin, M., Honrath, R.E., Owen, R.C., Lapina, K., 2008. Large-scale impacts of anthropogenic pollution and boreal wildfires on the nitrogen oxides over the central North Atlantic region. J. Geophys. Res. D Atmos. 113 http://dx.doi.org/10.1029/2007JD009689.

Val Martin, M., Logan, J.A., Kahn, R.A., Leung, F.-Y., Nelson, D.L., Diner, D.J., 2010. Smoke injection heights from fires in North America: analysis of 5 years of satellite observations. Atmos. Chem. Phys. 10, 1491–1510. http://dx.doi.org/10.5194/acp-10-1491-2010.

Van Der Werf, G.R., Randerson, J.T., Giglio, L., Collatz, G.J., Mu, M., Kasibhatla, P.S., Morton, D.C., Defries, R.S., Jin, Y., Van Leeuwen, T.T., 2010. Global fire emissions and the contribution of deforestation, savanna, forest, agricultural, and peat fires (1997–2009). Atmos. Chem. Phys. 10, 11707–11735. http://dx.doi.org/10.5194/acp-10-11707-2010.

Vermote, E., Ellicott, E., Dubovik, O., Lapyonok, T., Chin, M., Giglio, L., Roberts, G.J., 2009. An approach to estimate global biomass burning emissions of organic and black carbon from MODIS fire radiative power. J. Geophys. Res. D Atmos. 114 http://dx.doi.org/10.1029/2008JD011188.

Wang, P., Stammes, P., van der, A.R., Pinardi, G., van Roozendael, M., 2008. FRESCO+: an improved O2 A-band cloud retrieval algorithm for tropospheric trace gas retrievals. Atmos. Chem. Phys. 8, 6565–6576. http://dx.doi.org/10.5194/acp-8-6565-2008.

Wiedinmyer, C., Quayle, B., Geron, C., Belote, A., McKenzie, D., Zhang, X., O'Neill, S., Wynne, K.K., 2006. Estimating emissions from fires in North America for air quality modeling. Atmos. Environ. 40, 3419–3432. http://dx.doi.org/10.1016/j.atmosenv.2006.02.010.

Winkler, H., Sinnhuber, M., Notholt, J., Kallenrode, M.-B., Steinhilber, F., Vogt, J., Zieger, B., Glassmeier, K.-H., Stadelmann, A., 2008. Modeling impacts of geomagnetic field variations on middle atmospheric ozone responses to solar proton events on long timescales. J. Geophys. Res. 113, 11. http://dx.doi.org/10.1029/2007JD008574. D02302.

Wooster, M.J., Zhang, Y.H., 2004. Boreal forest fires burn less intensely in Russia than in North America. Geophys. Res. Lett. 31, L20505. http://dx.doi.org/10.1029/2004GL020805, 20501–20503.

Yokelson, R.J., Christian, T.J., Karl, T.G., Guenther, A., 2008. The tropical forest and fire emissions experiment: laboratory fire measurements and synthesis of campaign data. Atmos. Chem. Phys. 8, 3509–3527. http://dx.doi.org/10.5194/acp-8-3509-2008.

Web references

ftp://neespi.gsfc.nasa.gov/data/s4pa/Fire/MOD14CM1.005/ (last access August 2014).

https://lpdaac.usgs.gov/products/modis_products_table/mcd12q1 (last access August 2014).

ftp://ladsweb.nascom.nasa.gov/allData/51/MOD08_M3/2005/ (last access August 2014).

Please cite this article in press as: Schreier, S.F., et al., Differences in satellite-derived NO_x emission factors between Eurasian and North American boreal forest fires, Atmospheric Environment (2014), http://dx.doi.org/10.1016/j.atmosenv.2014.08.071